International Journal of Engineering

Journal Homepage: www.ije.ir

Probabilistic Seismic Assessment of Moment Resisting Steel Buildings Considering Soft-story and Torsional Irregularities

M. H. Razmkhah[a], H. Kouhestanian[b], J. Shafaei*[b], H. Pahlavan[c], M. Shamekhi Amiri[b]

[a] *Department of Civil Engineering Faculty, University of Semnan, Semnan, Iran*
[b] *Department of civil engineering, Shahrood University of Technology, Shahrood, Iran*

PAPER INFO

Paper history:
Received 03 August 2021
Received in revised form 19 September 2021
Accepted 23 September 2021

Keywords:
Incremental Dynamic Analysis
Probabilistic Seismic Assessment
Soft-story
Steel Moment Resisting Frame
Torsional Irregularity

ABSTRACT

In this study, the fragility curves were developed for three-, five-, and eight-story moment resisting steel frame structures with considering soft story and torsional irregularities during the earthquake mainshock to assess the probabilistic effects of irregularities in plan and height of steel structures. These models were designed according to Iranian seismic codes. 3D analytical models of steel structures were created in the OpenSees software platform and Incremental Dynamic Analysis (IDA) was conducted to plot the IDA curves. The maximum value of inter-story drift was selected as the demand parameter and the capacity is determined according to the HAZUS-MH limit states; finally, the corresponding fragility curves were developed. The results of the 3D nonlinear dynamic analysis indicated that the damage state of the structure due to soft story irregularity was decreased with increasing stories. On the other hand, the damage caused by torsional irregularity in plan was increased by increasing the height of the structure. For example, in the 3-story structure, soft-story effect on damage probability was more dominant than torsional irregularity.

doi: *10.5829/ije.2021.34.11b.11*

NOMENCLATURE

E	Steel module of elasticity (N/m^2)	PGA	Peak ground acceleration of ground motion (m/s^2)
I	Moment of inertia (m^4)	Δ	Lateral displacement (m)
K	Lateral stiffness (N/m)		

1. INTRODUCTION

Earthquake is one of the most destructive natural phenomena that can cause severe damages to the building structures, leading to huge economic damages and casualties. The disastrous economic and social consequences, which are resulting from inappropriate design and poor execution of buildings along with the expansion of the construction businesses, has highlighted the significance of proper design of structures, improvements and strengthening the buildings against earthquakes. Many buildings suffer from sudden changes to structural stiffness of stories because of including parking spaces, using buildings for commercial purposes and inappropriate usage of masonry infill walls, all of which create a soft or an extremely soft story condition that can lead to the vulnerability of buildings during earthquakes (Figure 1).

On the other hand, any irregularity in a plan like “mass eccentricity” may create torsion in the buildings which can cause the frame, on one side of building. This study focuses on examining the extent of damages to the structures with torsional irregularity in plan and soft story irregularity in height. Moreover, this study also examines the simultaneous effects of these two irregularities on the steel moment-resisting frame buildings.

The probabilistic seismic assessment of the existing steel buildings with the soft story and torsional irregularity is of great importance for presenting retrofitting plans and evaluating the vulnerability for

*Corresponding Author Institutional Email: j.shafaei@shahroodut.ac.ir (J. Shafaei)

Please cite this article as: M. H. Razmkhah, H. Kouhestanian, J. Shafaei, H. Pahlavan, M. Shamekhi Amiri, Probabilistic Seismic Assessment of Moment Resisting Steel Buildings Considering Soft-story and Torsional Irregularities, International Journal of Engineering, Transactions B: Applications, Vol. 34, No. 11, (2021) 2476-2493

Figure 1. Damages caused by soft-story irregularity in Kermanshah Earthquake, 2017

these types of structures. As a first step, the extent of damage to these types of structures should be detected and examined. Several studies have focused on the probabilistic seismic assessment of steel and reinforced concrete structures. The main focus of this study is to examine the effects of earthquakes on fragility curves of steel structures and to perform the probabilistic seismic assessment of steel structures constructed with regard to Iranian construction practice, according to Iranian Standard No. 2800, with soft story and plan torsional irregularities.

The increasing damages to the structures, caused by large and severe earthquakes such as 1994 Northridge earthquake in California, 1995 Kōbe earthquake in Japan and 2003 Bam earthquake in Iran, have highlighted the weaknesses of the existing codes of practice that are used for seismic design of buildings. In the current codes of practice, the structural designs are mainly performance-based and the displacement is regarded as the main criterion for designing the structures and detecting the magnitude of damage [1].

Initially, the fragility curves were used for analyzing the vulnerability of the nuclear power plants because the performance of these structures is of paramount importance and even the slightest defect may lead to disastrous incidents during earthquakes [2]. Therefore, the fragility curves were developed for the nuclear power plants with regard to different factors like Peak Ground Acceleration (PGA). These fragility curves were developed by Kircher and Martin [3]. After 1994 Northridge earthquake that caused huge financial damages to buildings, the engineering community majorly realized (focused on) the importance of assessing the extent of damages to the structures after severe earthquakes.

Anagnos and Rojahn [4] conducted several studies based on load distribution in ATC, all of which led to the development of a new type of fragility curve. In their study, all seismic calculations were conducted based on ATC-13. The horizontal axis of the fragility curves was the modified Mercalli values because it was a more scientific method for analyzing the fragility. Moreover, Log-normal distribution function was assumed in their study through which useful ideas were provided for future research regarding using earthquake records. They used the results of log-normal distribution for extracting the fragility curves.

Ozturk et al. [5] obtain seismic performance assessment for precast concrete industrial buildings using the fragility curves.

Naseri and Ghodrati [6] applied the fragility curves to examine the reinforced concrete structures without considering the effect of infilled frame and the structural vulnerability. The results indicated that the slope of fragility curve was higher at slight and moderate damage states and at low PGA. As PGA values increased, the slope of the fragility curve decreased i.e. the probability of damage was higher at lower PGA values [7].

In 2017, Ouzturk [8] estimated the seismic behavior of two monumental buildings in the historical Cappadocia region of Turkey, and It was observed that slab discontinuities on the first floors constitute a major element in the expected structural damage for both buildings. In addition, upon application of certain ground motions, destructive levels of drift were observed, another element contributing to the expected damage.

Hwang and Lee [9] examined the effect of assigned risk category on the earthquake performance of low- to mid-rise, steel special moment-resisting frame (MRF) buildings. The results indicated that the collapse risk of the steel special MRF buildings of an ordinary occupancy used showed in earthquake much higher than that of the higher risk buildings.

Moufid Kassem et al. [10] used Group of National Defense against earthquake (GNDT) approach for seismic performance assessment and the results indicated that there is a good correlation between the analytical modeling approach and the observed fragility features during in-situ field investigations.

Fattahi and Gholizadeh [11] assessed the seismic performance of the reinforced Steel Moment Frames (SMFs) under performance-based design (PBD) framework. For this purpose, SMFs were optimized. Then the optimized SMFs were analyzed using incremental non-linear dynamic analysis (IDA). Later, the fragility curves were plotted to examine the damage states. The results indicated that the design optimization could only be efficient before the structure faced the complete collapse state.

Taiyari et al. [12] investigated on damage-based optimal design of friction dampers in multistory chevron braced steel frames. The performance of proposed method was illustrated using three steel moment-resisting frames models with friction damper systems such as chevron braces and damper devices. According to the results, the largest damage probability in every structural model was associated with higher slip force and the lower stiffness ratio, where the undesirable buckling failure occurred before the friction damper was fully activated.

The main purpose of this study is to examine the effects of soft-story and torsional irregularities of steel moment-resisting frames on the four damage states during earthquakes, with respect to HAZUS-MH MR-5 code [13]. Therefore, fragility curves are developed for four damage states to examine the effect of soft-story irregularity on the lateral load stiffness of the first-story and to investigate the effect of the torsional irregularity in plan on the 3, 5, and 8 story steel moment-resisting frame models during the earthquake.

The soft-story irregularity can occur for several reasons such as inappropriate usage of masonry infill walls, increasing the height of the structure or removing a structural element (column or beam) to create parking spaces. In this study, the main reason for soft-story irregularity was attributed to the increase of height in buildings which in turn led to the reduction of Lateral Load Stiffness. Moreover, torsional irregularity can occur as a result of asymmetric usage of lateral load resisting systems, the existence of large openings in the diaphragm, plan asymmetry and excessive concentration of gravity load on one side of plan, etc. The irregularity caused by the asymmetry in the lateral load resisting systems is also examined in this study.

2. INTRODUCTION OF THE MODELS (BUILDING STRUCTURES) OF THE STUDY

The 3D models used in this study have consisted of three-, five- and eight-story buildings with medium steel moment frames as their lateral load resisting systems, the characteristics of which are as follows:

A) Structures with regularity in plan and height (Figure 2(a))

B) Structures with regularity in plan and soft-story irregularity

C) The structure with simultaneous soft-story irregularity and torsional irregularity in plan (Figure 2(b))

The buildings were designed in accordance with the existing standard codes of Iran. The characteristics of the model that is used in this study are as follows:

- The structure is built on relatively high seismic hazard zones.
- The soil of construction site is considered to be Type III.
- The height of the first story is considered to be 2.8 and 3.8 m for the structure with regular height and soft story irregularity, respectively. The heights of other stories are considered as 3.2 m.
- The steel's yield stress which is used in the beam and column equals 240 MPa.
- The steel's ultimate stress that is used in the beam and column equals 370 MPa.

3. DETECTING SOFT STORY AND TORSIONAL IRREGULARITY

According to Iranian Standard No. 2800, the soft story condition occurs when the lateral stiffness of one story of the building is 70% lower than the upper stories. Torsional irregularity occurs when the ratio of maximum story displacement is 1.2 times greater than the average story displacement of the structure. In this study, the lateral stiffness of the first story is calculated using the Etabs software program. Moreover, the stiffness of the first and other stories was compared to detect soft-story irregularity.

In Etabs, a unit load (F) was applied on the diaphragm of the first story and the drift of the first story was calculated to estimate the story's stiffness using Equation (1). The value of K is equal to the lateral stiffness of the structure and Δ the lateral displacement of the structure.

Then, the stiffness of the second story was computed. In order to detect the existence of soft stories in the first story, the stiffness of the first and second stories was compared by considering the fact that soft-story condition occurs when the stiffness of the first story is 60 to 70% lower than the second story.

In order to determine the torsional irregularity of the structure, firstly, the maximum and average displacement of the structure were separately calculated. Then, the ratio of the maximum and average displacement was estimated. Torsional

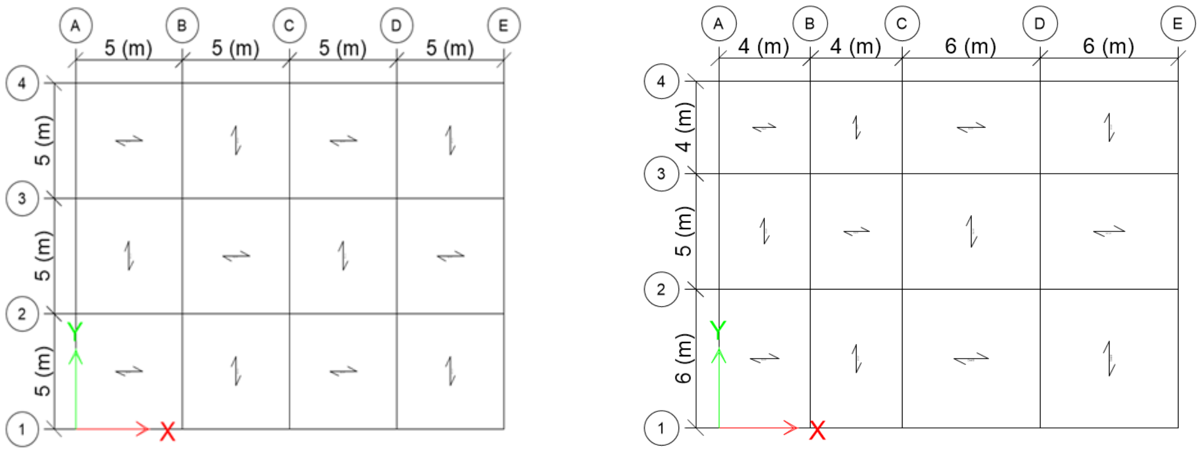

Figure 2. The plan of different types of modeled structures: (a) Structure with regular plan; (b) Structure with an Irregular plan

irregularity occurs if the ratio of maximum story displacement is 1.2 times greater than the average story displacement of the structure (Standard No. 2800 of Iranian code [14]).

In addition to utilize Etabs to calculate the lateral stiffness of the structure, Equation (2) can be used to estimate the lateral stiffness of each story. In this relation E is the modulus of elasticity and I is the moment of inertia as well as L is the length of the column.

$$F = K\Delta \quad (1)$$

$$K = \sum \frac{12EI}{L^3} \quad (2)$$

After calculating the lateral stiffness of the models under this study, it can be concluded that if the height of the first story is 3.8 m, the stiffness of the first story will be 61% lower than that of the second story; and consequently, the first story has soft story irregularity.

4. OPENSEES SOFTWARE VERIFICATION WITH EXPERIMENTAL RESULTS

The first step in modeling software is to validate the results obtained through software with the actual behavior of the structure. Figure 3 shows a 4-story, 2-span frame prototype model of an office building in the Los Angeles area. The structural system of this prototype model consisted of the lateral load system of special moment-resisting frame (SMRF) with reduced beam sections (RBS). The soil type D was used in the construction site. This model was comprised of two spans, columns axis-to-axis length of 9100 mm, first story height of 4600 mm and other stories are of 3700 mm high.

This model was designed based on IBC [15]. The gravity loads and lateral load are calculated and applied on the structure based on ASCE-7 [16] and AISC [17], respectively.

The beam sections that were used in the first and second stories and also in the third and fourth stories were W27X102 and W21X93, respectively. The column's sections which were used in the first and second stories and also in the third and fourth stories were W24X131 and W24X76, respectively. A992 steel Grade 50 was used in all elements of this model. The lateral loads that were applied on the first three stories and on the fourth story were assumed as 4600N and 5300 N (1200 Kips), respectively [18]. As can be seen in Figure 4, in order to compare the results that were obtained by the experimental and software models, the load-drift curves were developed for both models. For analytical model, Uniaxial Materials Command is used to define steel materials [8]. In this study, the Steel02 materials with isotropic' hardening are used; because these materials also take rupture and the drop resistance conditions into consideration as well [19]. Fiber Section was used to define the beam and column cross-sections in OpenSees and can be used to apply

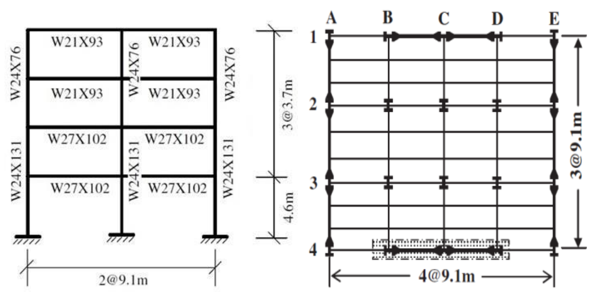

Figure 3. The details of 2D frame used for verification [19]

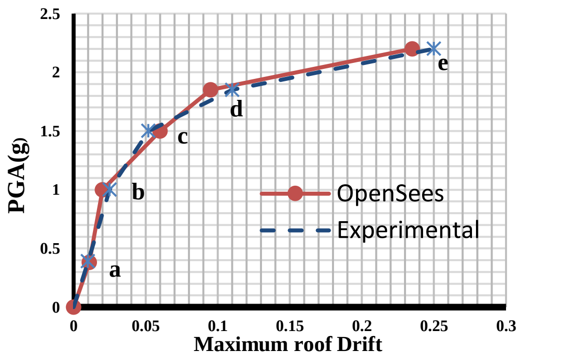

Figure 4. The comparison between Load-displacement curves of experimental and OpenSees samples

different characteristics of the materials to every cross-section of the element.

Since the non-linear analysis was applied in this study, Nonlinear Beam-Column Element command was used to define the elements. The elements are modeled non-linearly by using this command. Moreover, this command is also used to distribute the inelastic effects throughout the model. The experimental sample was modeled in OpenSees after selecting and examining the behavior model of the material in this software. The gravity and lateral loads were applied on the OpenSees sample with respect to the experimental sample. Accordingly, the roof displacement of OpenSees sample that was obtained from PGA, was extracted. Figure 4 illustrates the load-displacement curves of experimental and OpenSees samples.

As shown in Figure 4, relatively similar results, with high level of accuracy, were obtained for both experimental and modeled results.

5. ACCELEROGRAPH SELECTION

One of the most significant steps in the non-linear dynamic analysis is determined the ground-motion records because the results obtained by incremental dynamic analysis (IDA) are mainly dependent on these records. The records must be selected in such a way as to include all seismic behaviors of the structure. In this study, 20 ground-motion records are selected from "Peer" website while considering the soil type of the site and Li et al. [20] suggestions as follows:

- The shear velocity of the soil must be 175-375 m/s, with regard to the site's soil type.
- The Peak Ground Acceleration (PGA) must be greater than 0.4 g.

The selected records are summarized in Table 1.

TABLE 1. Selected Records

Record No	Record name	Site name	Soil type	Earthquakes Magnitude (Richter)	PGA(g)
1	Chalfant valley	Zack Brothers Ranch	III	6.19	0.447
2	Coalinga	Oil-City	III	5.77	0.398
3	Northridge	Sun Valley - Roscoe Blvd	III	6.69	0.604
4	Imperial Valley	El Centro Array #11	III	6.53	0.37
5	Coalinga	14Th & Elm (Old CHP)	III	5.77	0.84
6	Imperial Valley	Bonds Corner	III	6.53	0.776
7	Mammoth lakes	Convict Creek	III	6.06	0.444
8	Mammoth lakes	Fish & Game (FIS)	III	5.94	0.376
9	Mammoth lakes	Mammoth Lakes H. S	III	5.69	0.44
10	Managua-Nicaragua	Managua-Esso	III	6.24	0.371
11	Northridge	Northridge - 17645 Saticoy St	III	6.69	0.459
12	Northridge	Canoga Park - Topanga Can	III	6.69	0.392
13	Northridge	Jensen Filter Plant Administrative Building	III	6.69	0.617
14	Northridge	La - Sepulveda Va Hospital	III	6.69	0.93
15	Northridge	Newhall - Fire Sta	III	6.69	0.59
16	Northridge	Rinaldi Receiving Sta	III	6.69	0.87
17	Imperial Valley	El Centro Array #4	III	6.53	0.48
18	Imperial Valley	El Centro Array #5	III	6.53	0.53
19	Imperial Valley	El Centro Array #7	III	6.53	0.57
20	Imperial Valley	El Centro Array #8	III	6.53	0.61

In this study, in order to develop the fragility curves and to also compare the damages to the structures, all accelerograph records of the main-shock were scaled up to 1g. A sample of motion records recovered from the Mammoth Lakes-Convict Creek earthquake is shown in Figure 5.

6. HYSTERESIS CURVE

The moment-rotation hysteresis curve was examined to investigate the performance of the model and cross-sections built in OpenSees. The selected beam's hysteresis curve is shown in Figure 6. The hysteresis curve of the beam in the first story under the Chalfant valley earthquake in Zack Brothers Ranch site is shown in Figure 7 while the hysteresis curve of the column in the first story under the earthquake that was scaled up to 1g.

Figure 8 shows the column hysteresis curves along the C-2 axis, in the first story under Chalfant valley earthquake in Zack Brothers Ranch site; and also under the earthquake that was scaled up to 1g, which are shown in Figure 9. As shown in Figure 9, there is a slight difference in the amount of energy absorption for the column specified in the five-story structure with the soft story and with the soft story and torsional irregularity for the specified record.

After examining the hysteresis curves, it was observed that beam and column elements entered in the inelastic region which highlights the capability of the analysis model in estimating the structural non-linear response.

7. COMPARISON OF BASE SHEAR OF THE MODELS

One of the most important curves of the seismic behaviors of the structures is known as the base

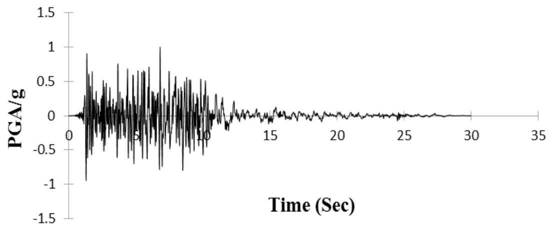

Figure 5. The scaled accelerographs of Mammoth Lakes-Convict Creek earthquake

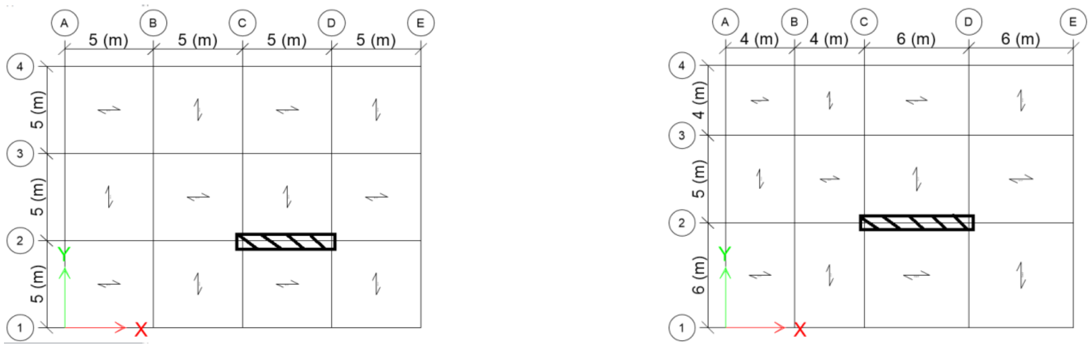

(a) (b)

Figure 6. The beam selected for plotting hysteresis curve: (a) The 5-story structure with soft story irregularity (b)The 5-story structure with soft story and torsional irregularity

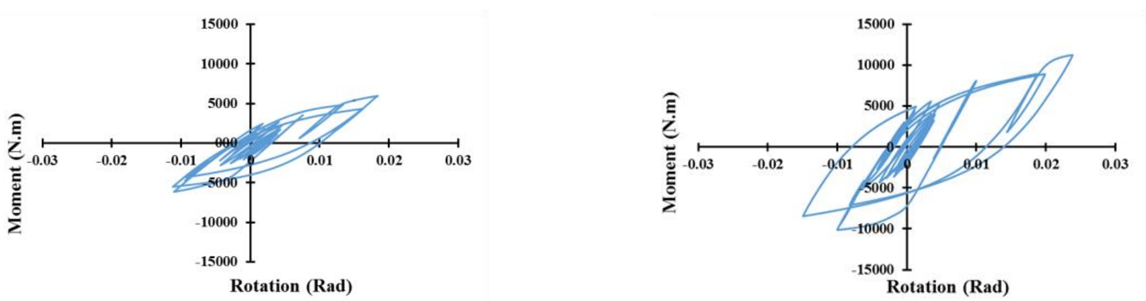

(a) (b)

Figure 7. The moment-rotation hysteresis curve of beam in the 5-story structure: (a) Structure with soft story irregularity; (b) Structure with soft story and torsional irregularity

shear-roof displacement curve, through which the stiffness variations of the structure, the structure strength, and ductility are demonstrated. Figure 10 represents the base shear-roof displacement curves of 3, 5 and 8-story structures. There is little difference between the base shear-roof displacement curve of the three-story structure with a soft story and the three-story structure with simultaneous a soft story and torsional irregularity. The reason for this phenomenon can be stated in the fact that due to the low height of the structure, the amount of displacement of the roof of the structure to the base shear force is not sensitive to the existence of soft story and torsional irregularities in the structure. After comparing the effects of torsional and soft-story irregularities on the base shear-roof

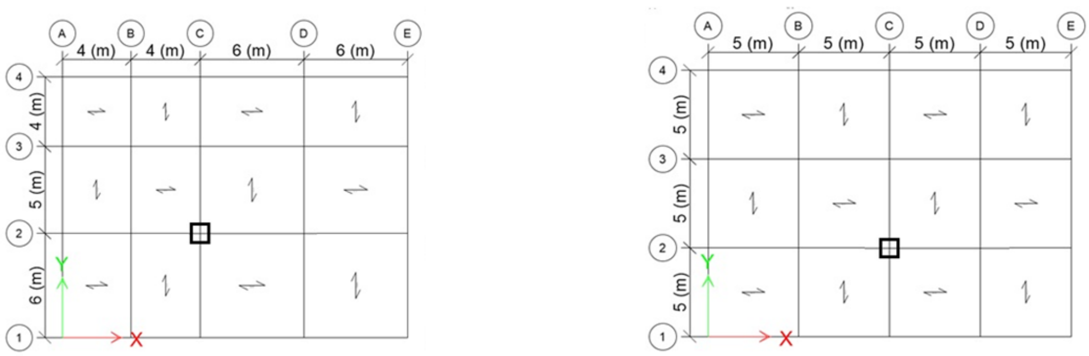

(a) (b)

Figure 8. The column selected for plotting hysteresis curve: (a) The 5-story structure with soft story irregularity; (b) The 5-story structure with soft story and torsional irregularity

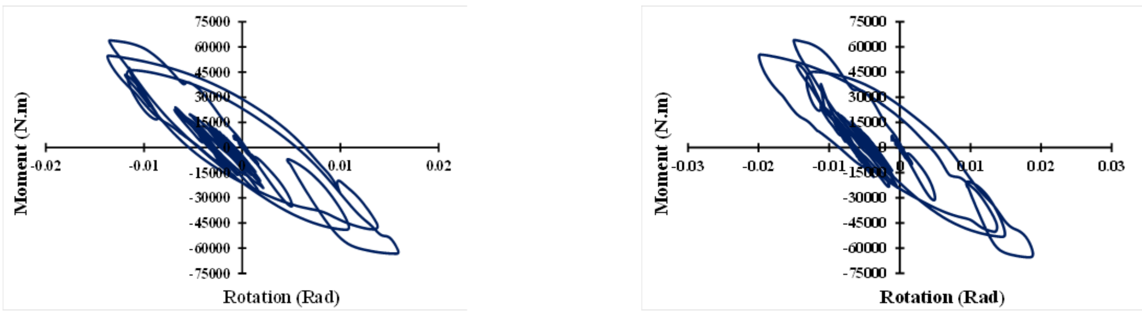

(a) (b)

Figure 9. The moment-rotation hysteresis curve of column in the 5-story structure**:** (a) Structure with soft story irregularity; (b) Structure with soft story and torsional irregularity

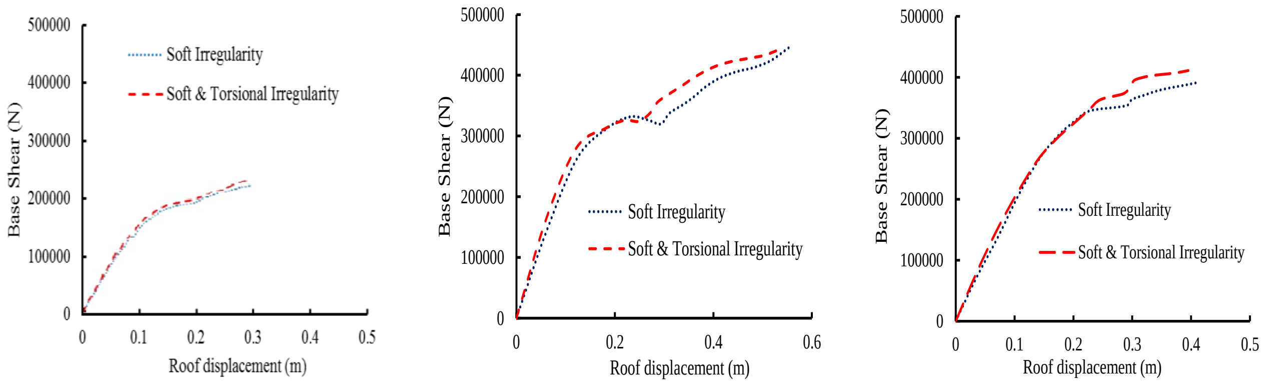

(a) (b) (c)

Figure 10. The base shear-roof displacement graph: (a) 3-story structures (b) 5-story structures (c) 8-story structures

displacement graphs, it was indicated that the shear-base increased in equal displacements in the structures with torsional irregularity. In fact, the shear-base values increased up to 7, 9 and 11% in the 3, 5 and 8-story structures, respectively.

8. COMPARING THE INCREASE OF DRIFTS AMONG THE STRUCTURES

The building structures may be affected by the earthquakes with different magnitudes during over different periods of time. Therefore, Figure 11 represents the comparison among the drifts of the structures in this study for three different PGA values, 0.1g, 0.2g, 0.3g, under Chalfant valley earthquake in Zack Brothers Ranch site (See Figures 11, 12 and 13).

After comparing the drift graphs of 3, 5 and 8-story structures, it was observed that on the roof level, the drift in the structures with simultaneous soft story and torsional irregularities was greater than that of the structures with only soft-story irregularity. The drift evidently increased with an increasing the number of stories, (The increase in drift became more evident with increasing number of stories).

The effects of the earthquakes on the drifts of different stories and various movement modes of the structures can be observed after comparing the story drifts of the structures with different heights. The movement mode was similar in the structure with the same number of stories but different types of irregularities. Although the movement mode of the structure is dependent on the number of stories, but it is not affected by different types of regularities.

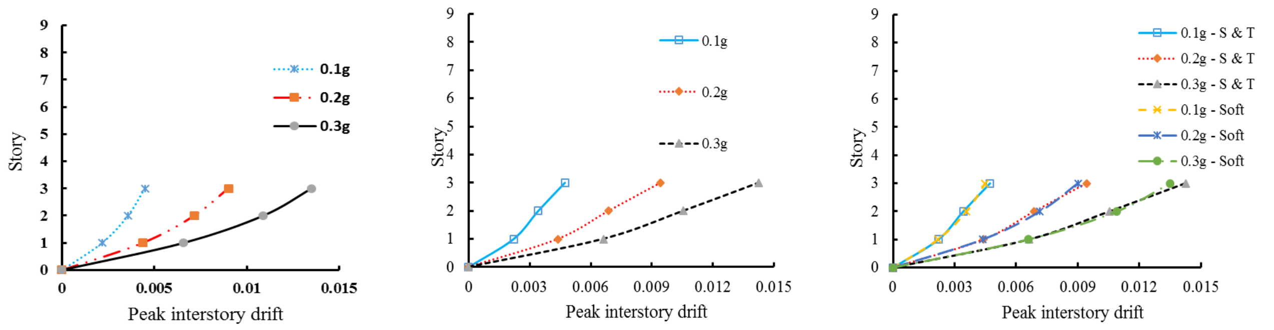

(a) (b) (c)

Figure 11. The drift graph of 3-story structures: (a) only the soft-story irregularity (b) Simultaneous soft story and torsional irregularities (c) The drift graph of 3-story structures with only the soft-story irregularity and also simultaneous soft story and torsional irregularities

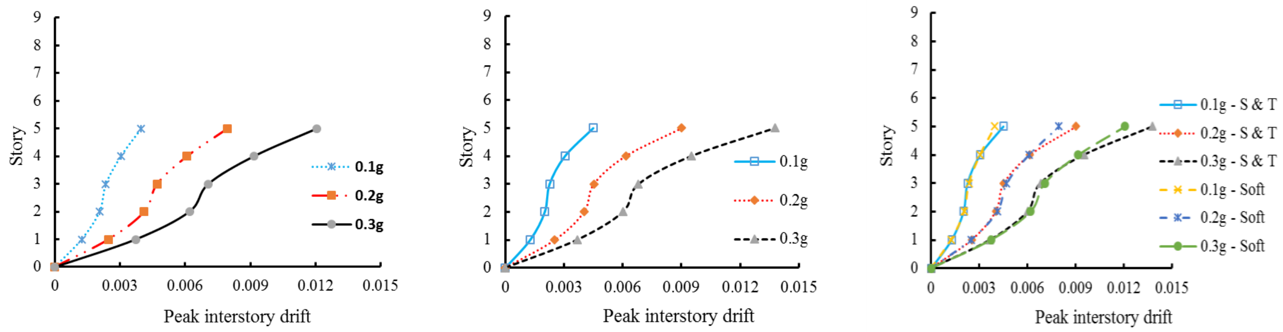

(a) (b) (c)

Figure 12. The drift graph of 5-story structures: (a) only the soft-story irregularity (b) Simultaneous soft story and torsional irregularities (c) The drift graph of 5-story structures with only the soft-story irregularity and also simultaneous soft story and torsional irregularities

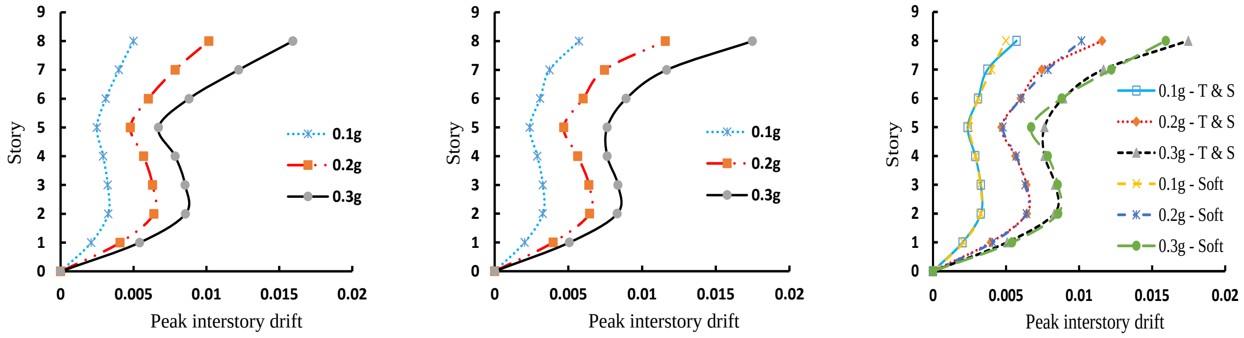

(a) (b) (c)

Figure 13. The drift graph of 8-story structures: (a) only the soft-story irregularity (b) Simultaneous soft story and torsional irregularities (c) The drift graph of 8-story structures with only the soft-story irregularity and also simultaneous soft story and torsional irregularities

9. COMPARISON AMONG THE ROOF DISPLACEMENT OF STRUCTURES DURING EARTHQUAKES

In order to compare the displacement of structures in this study during earthquakes and also observe their permanent displacements, these structures were examined under Chalfant valley records in Zack Brothers Ranch site.

As can be seen in Figure 14, since relatively identical roof displacements were observed in the three-story structures with different irregularities, their permanent displacements were also similar to one another. However, in five-story structures (Figure 15), a small roof displacement was observed in structures with simultaneous soft story and torsional irregularity. Therefore, the permanent displacement of the five-story structure with simultaneous soft story and torsional irregularity was smaller than that of with soft story irregularity. On the other hand, identical permanent displacements were observed in eight-story structures with both soft story irregularity and simultaneous soft story and torsional irregularity (Figure 16).

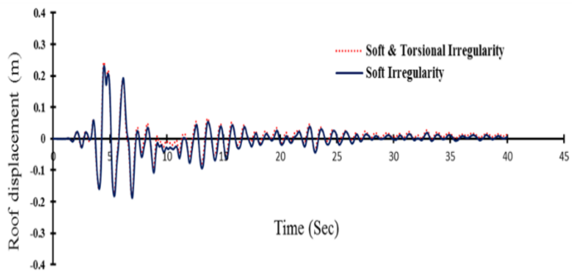

Figure 14. The roof displacement graph during earthquake in two 3-story structures with soft story irregularity and simultaneous soft story and torsional irregularities

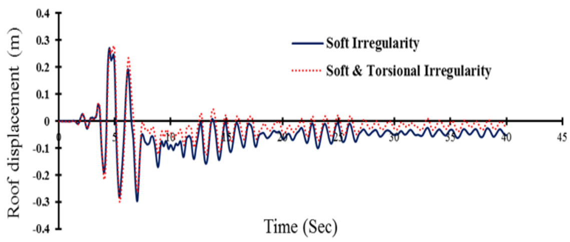

Figure 15. The roof displacement graph during earthquake in two 5-story structures with soft story irregularity and simultaneous soft story and torsional irregularities

10. THE INTRODUCTION OF DAMAGE STATES

Four damage states including slight, moderate, extensive and complete collapse are introduced for the structure with respect to HAZUS-MHMR-5. Table 2 shows the maximum displacement of each damage state. According to HAZUS-MHMR-5, the point at which the materials reach the softening region to achieve the complete dynamic instability is considered as the best point in which the structure can withstand until the complete collapse occurs.

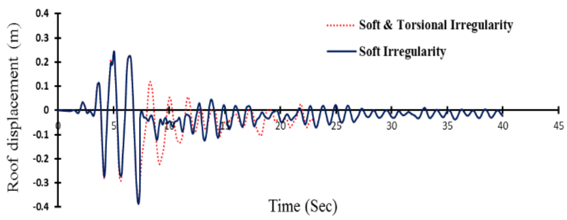

Figure 16. The roof displacement graph during earthquake in two 8-story structures with soft story irregularity and simultaneous soft story and torsional irregularities

This point has the slightest damage state among other points. Another damage criterion is known as the maximum drift among the stories. Table 2 shows the maximum drifts of low-, mid- and high-rise structures with respect to HAZUS-MH MR-5 code.

11. IDA CURVES FOR SOME MODELS IN THIS STUDY

Incremental dynamic analysis is a seismic analysis method based on the structures' performances. The structures' behaviors with different intensity levels are also identified by IDA. Unlike pushover analysis, IDA can be successfully used to determine the structural capacity, the collapse probability and the percentage of reaching a particular damage limit. IDA provides more precise analyses, compared to the pushover method due to have some capabilities such as introducing the materials with non-linear behaviors and performing dynamic analyses [21].

TABLE 2. The amount of drift at different damage states considering the damage type considering HAZUS-MHMR-5

Structure type	Drift at the Threshold of damage state			
	Slight damage	**Moderate damage**	**Extensive damage**	**Complete damage**
Low-rise	0.006	0.00104	0.0235	0.06
Mid-rise	0.004	0.0069	0.0157	0.04
High-rise	0.003	0.0052	0.0118	0.03

In this study, IDA was used to examine the models in such a way that the maximum PGA, applied on the structure, was scaled up to 0.1g. Then, IDA curves were developed after analyzing the structure at each incremental PGA value. In this study, IDA curves were developed for three, five and eight-story structures, under the main-shock and also the main-shock-aftershock sequence under 20 accelerographs in Figures 17, 18 and 19.

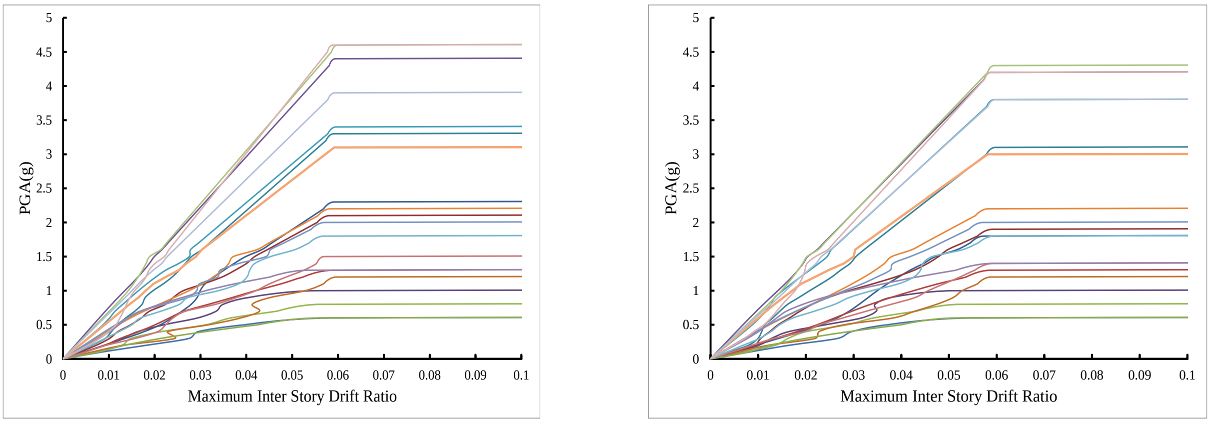

(a) (b)

Figure 17. IDA graph (curve) for 3-story structure: (a) With soft story irregularity (b) With soft story and torsional irregularity

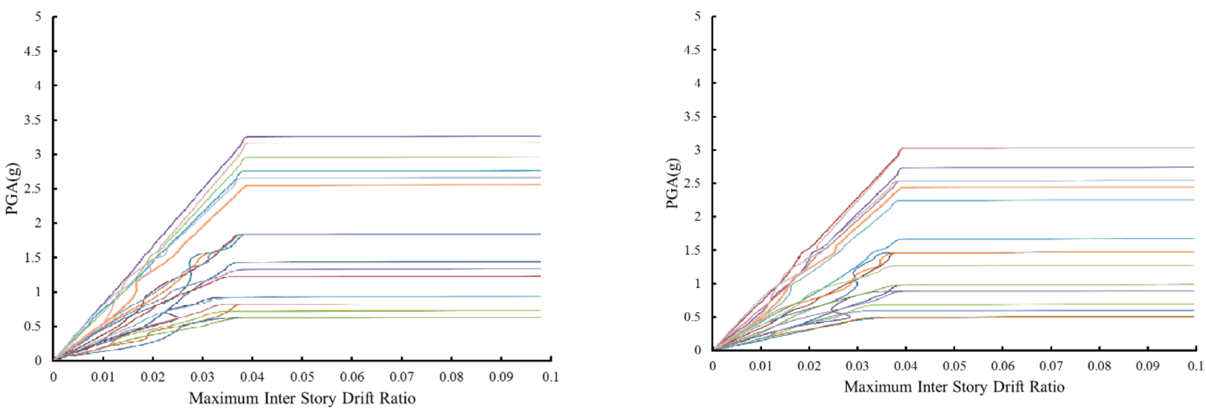

(a) (b)

Figure 18. IDA graph (curve) for 5-story structure: (a) With soft story irregularity (b) With soft story and torsional irregularity

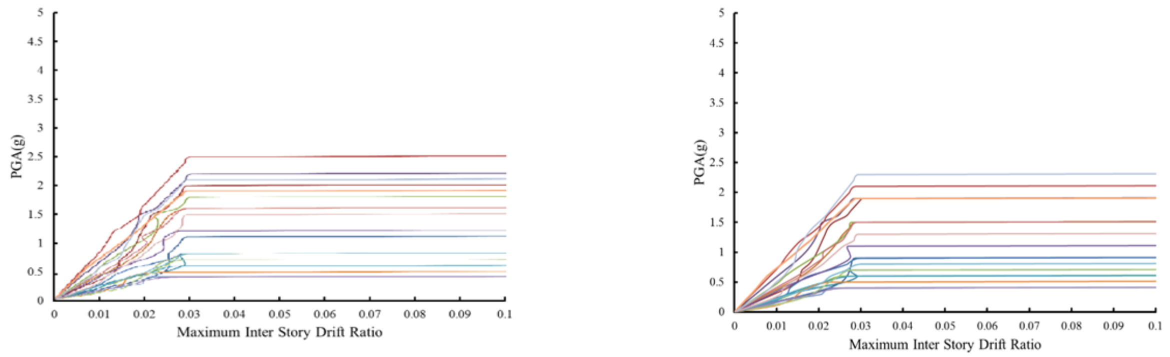

(a) (b)

Figure 19. IDA graph (curve) for 8-story structure: (a) With soft story irregularity(b) With soft story and torsional irregularity

Considering the IDA graphs, it can be concluded that the structures exhibited extreme load resistance behavior under accelerographs, indicating that the displacement hardly occurred in the structure and mostly appeared around the slope of the elastic region. Moreover, a relatively constant increase was observed in the relative drift of three-story structures. However, as the number of stories increased, the drift of some stories led to the complete collapse of the structure.

12. DEVELOPING AND PLOTTING THE FRAGILITY CURVE

The fragility curves are considered as one of the useful tools for analyzing the damage probability of the structures. The probability of exceedance from a particular damage state against seismic parameters of the structure is determined through fragility curves. While developing the fragility curves, it should be noticed that the characteristics of the structures are different in every country. Therefore, the specific characteristic of every structure should be taken into consideration for analysis process. A probability distribution for engineering demand parameter, obtained from IDA, was used to develop a fragility curve.

This study used the Log-normal distribution to develop the fragility curves. Every structure was analyzed under 20 ground motion records, the PGA values of which varied from 0.1g to 1.5g. Then, the fragility probability of the structure was examined using OpenSees. Since the structural capacity and seismic demand are the two parameters that follow the log-normal distribution. Therefore, the fragility curves can be developed as a cumulative lognormal distribution function, based on Equation (3):

$$P(:\leq D)=\Phi\left[\left(\frac{\mathrm{Ln}\left(S_d/S_c\right)}{\beta_{sd}}\right)\right] \quad (3)$$

P is considered as the probability of reaching to or exceeding the *damage state (D) (the maximum inter-story displacement),* β_{sd} is the standard deviation of Log-normal distribution, s_c is the mean value of capacity limit state and S_d is the median value of seismic demand.

Figure 20 shows the fragility curves of four damage states in the three-story structure with regularity in plan and height, with simultaneous soft story and torsional irregularity, and with only soft story irregularity under ground motion records.

Figure 21 illustrates the fragility curves of four damage states in the five-story structure with regularity in plan and height, with simultaneous soft story and torsional irregularities, and with only soft story irregularity under ground motion records.

Figure 22 depicts the fragility curves of four damage states in the for eight-story structure with regularity in plan and height, with simultaneous soft story and torsional irregularity, and with only soft story irregularity under ground motion records.

13. THE COMPARISON AMONG THE FRAGILITY CURVES OF THE STRUCTURES

In this section, the fragility curves of three-, five- and eight-story structures are investigated.

13. 1. Comparison among the Fragility Curves of the three-story Structure

Firstly, the fragility curves of 3, 5 and 8-story structures with regularity in plan and height, with simultaneous soft story and torsional irregularity, and with only soft story irregularity during the earthquake were separately calculated and developed. Then, the fragility curves of the structure with regularity in plan and height were compared with that of the structure with soft story irregularity. Later, the fragility curves of structures with only soft story irregularity were compared with that of the structures with simultaneous soft story and

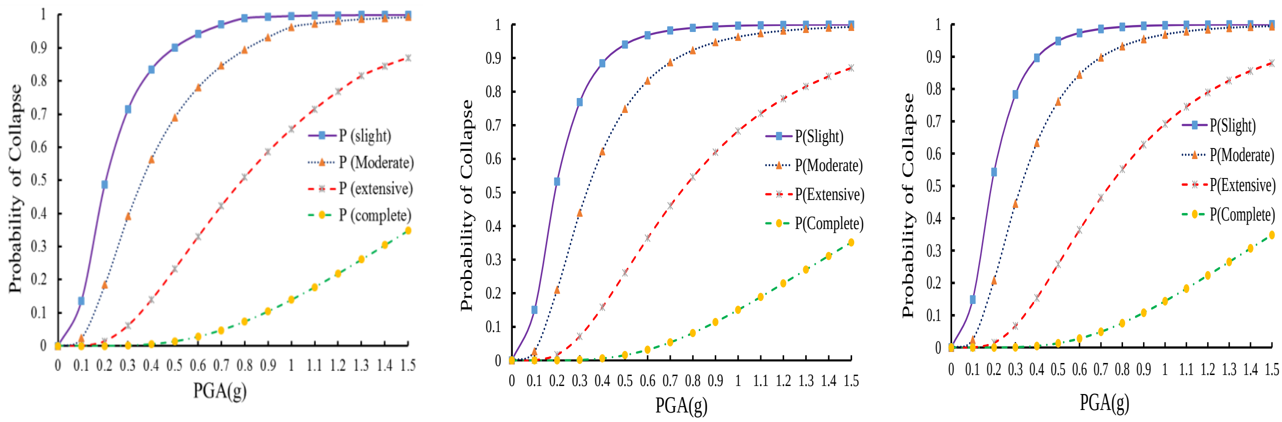

(a) (b) (c)

Figure 20. Fragility curve of 3-story structure: (a) Structure with regularity in plan and height (b) Structure with soft story irregularity (c) Structure with simultaneous soft story and torsional irregularity

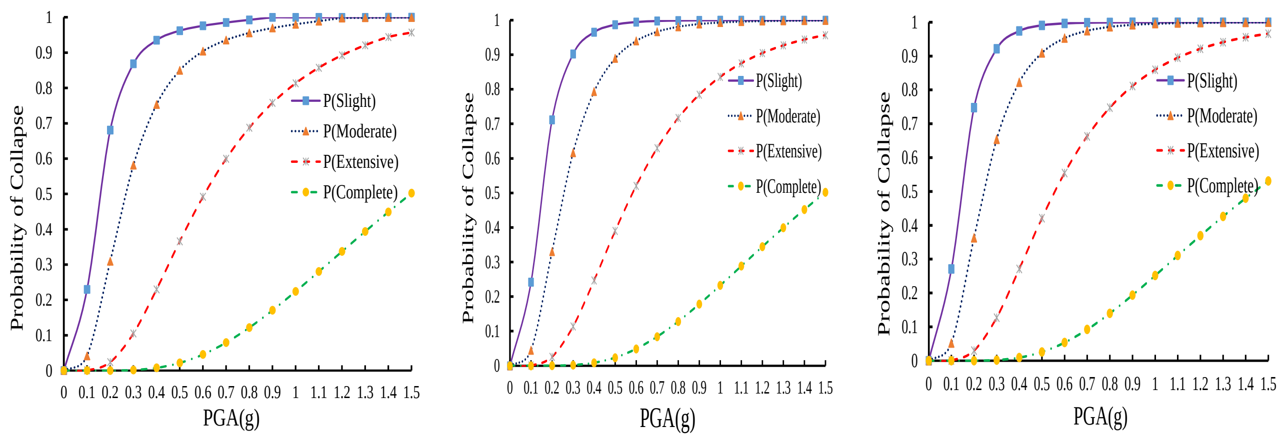

(a) (b) (c)

Figure 21. Fragility curve of 5-story structure: (a) Structure with regularity in plan and height (b) Structure with soft story irregularity (c) Structure with simultaneous soft story and torsional irregularity

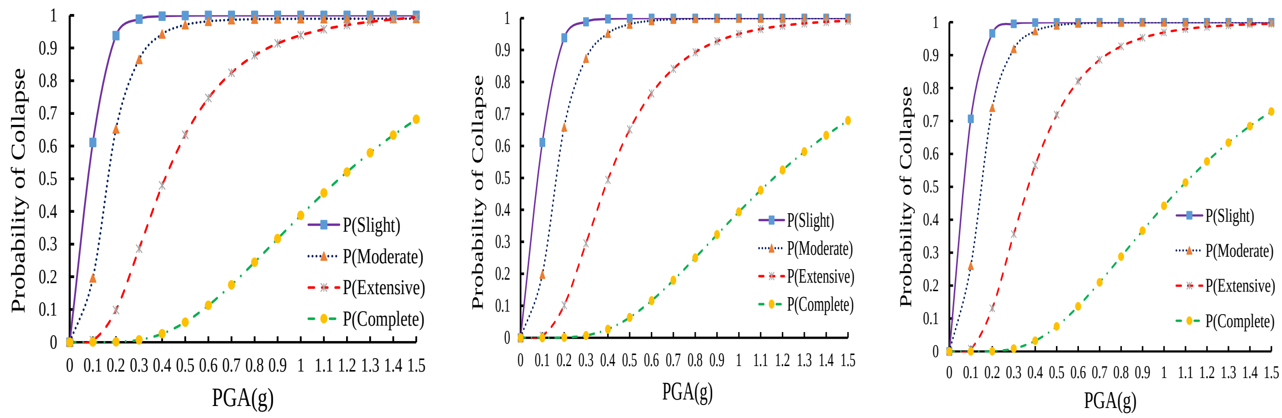

(a) (b) (c)

Figure 22. Fragility curve of 8-story structure: (a) Structure with regularity in plan and height (b) Structure with soft story irregularity (c) Structure with simultaneous soft story and torsional irregularity

torsional irregularity under the given earthquake. Firstly, Figure 23 demonstrates the comparison among 3-story structure with different irregularities.

After comparing the 3-story structure with soft story irregularity and with regularity in plan and height, it was concluded that when the structure was put under ground motion records, the PGA values of structure with soft-story irregularity decreased to almost 5, 8 and 9% to the midpoint of slight, moderate, extensive damage states, respectively; compared to structure with regularity in plan and height. As for the complete collapse state, the PGA value of the structure with soft-story irregularity decreased to 4%, compared to the structure with regularity in plan and height which led to 20 % probability of the complete collapse of the structure.

After comparing the 3-story structure with soft-story irregularity and with simultaneous soft-story and torsional irregularity, it was observed that in both models, the midpoint fragility values occurred at relatively equal PGAs. Therefore, the fragility curve of the structure with soft-story irregularity was relatively compatible with that of the structure with simultaneous soft-story and torsional irregularity.

13. 2. Comparison among the Fragility Curves of the Five-story Structure This part focused on comparing the fragility curves of the 5-story structure under ground motion records (Figure 24).

After comparing the 5-story structure with soft story irregularity and with regularity in plan and height, it was observed that when the structure was put under different ground motion records, the PGA of the structure with soft-story irregularity decreased to almost 3, 4 and 5% to the midpoint of slight, moderate, extensive damage states; respectively; compared to structure with regularity in plan and height. As for the complete collapse state, the PGA value of the structure with soft-story irregularity decreased to 3%, compared to that of the structure with regularity in plan and height which led to 20% probability of complete collapse of the structure.

After comparing the 5-story structure with soft-story irregularity and with simultaneous soft-story and torsional irregularity, when the structure was put under different ground motion records, the PGA of structure with simultaneous soft-story and torsional irregularity decreased to almost 3, 4, 5 and 6% to the midpoint of slight, moderate, extensive damage states and complete collapse, respectively; compared to that of the structure with only soft-story irregularity.

13. 3. Comparison among the Fragility Curves of the 8-story Structure After developing and comparing the fragility curves of 3 and 5-story structures under different ground motion records, finally, the fragility curves of 8-story structures under ground motion records were also compared (Figure 25).

After comparing the 8-story structure with soft story irregularity and with regularity in plan and height, it was observed that when the structure was put under different ground motion records, the two structures had relatively equal PGAs to the midpoints of slight and moderate damage states. As a result, the fragility curve of the 8-story structure with soft story irregularity was compatible with that of the structure with regularity in plan and height. Moreover, the PGA of the structure with soft story irregularity decreased to 2 and 3% to the midpoint of the extensive and complete collapse, respectively; compared to that of the structure with regularity in plan and height.

After comparing the 8-story structure with soft-story irregularity and with simultaneous soft-story and torsional irregularity, it was concluded that when the structure was put under different ground motion

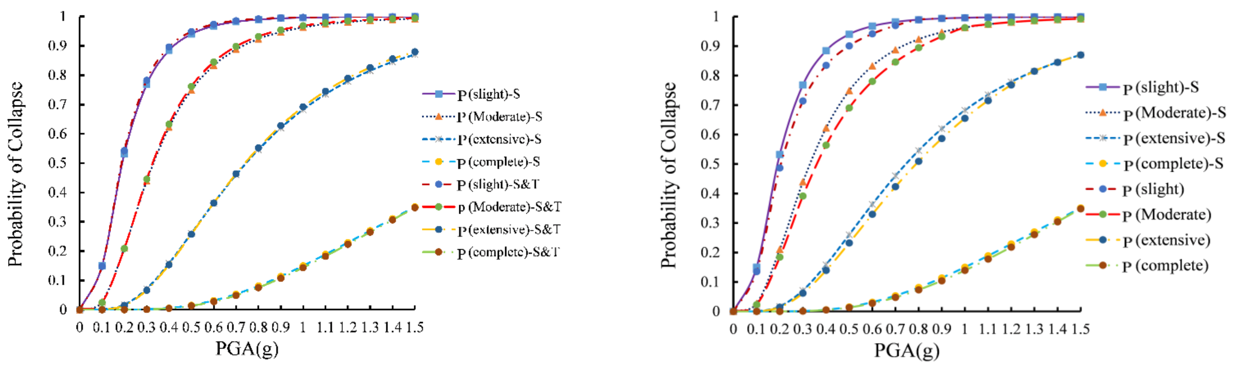

(a) (b)

Figure 23. Fragility curve of 3-story structure: (a) With soft story irregularity (b) With simultaneous soft story and torsional irregularity

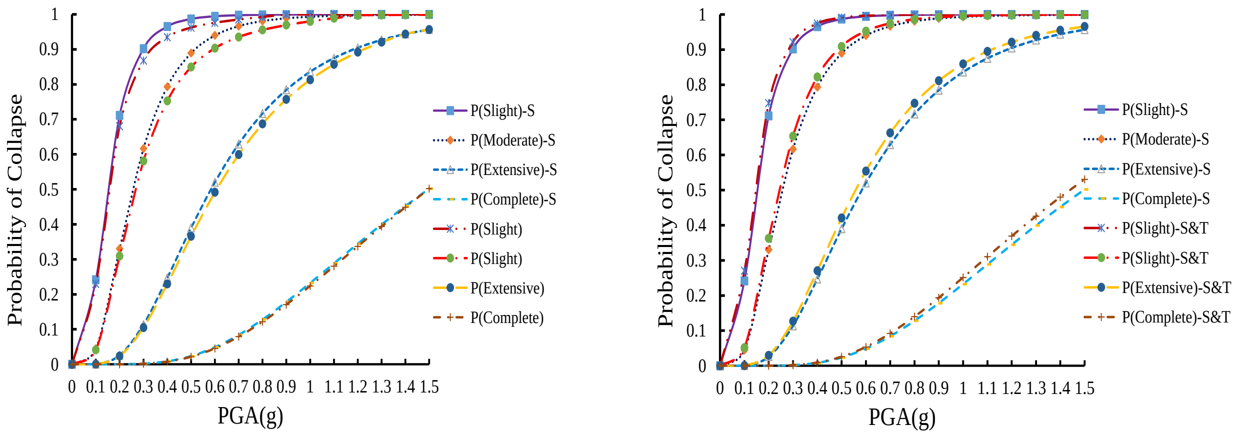

(a) (b)

Figure 24. Fragility curve of 5-story structure: (a) With soft story irregularity (b) With simultaneous soft story and torsional irregularity

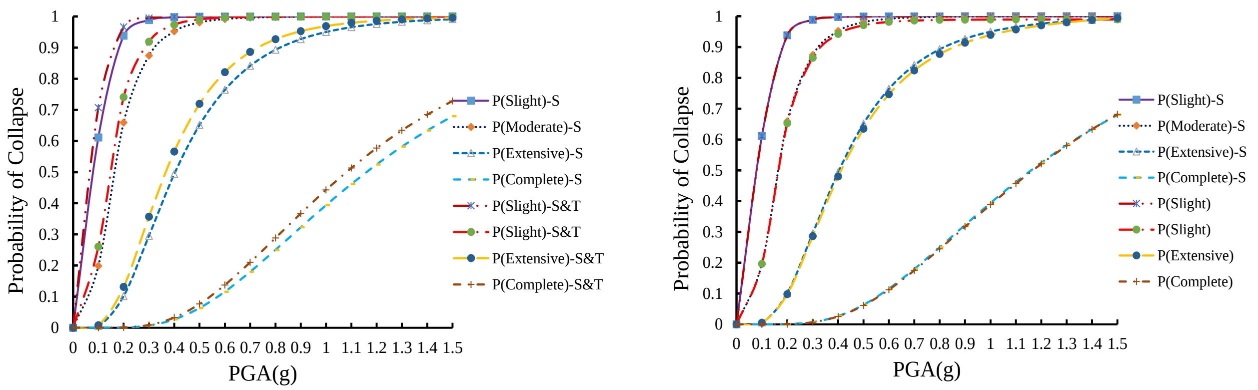

(a) (b)

Figure 25. Fragility curve of 8-story structure: (a) With soft story irregularity (b) With simultaneous soft story and torsional irregularity

records, the PGA of structure with simultaneous soft-story and torsional irregularity decreased to almost 15, 12, 10 and 9% to the midpoint of slight, moderate, extensive damage states and complete collapse, respectively; compared to that of the structure with soft-story irregularity.

14. CONCLUSIONS

After analyzing the three, five and eight-story steel structures with regularity in plan and height, with only soft-story irregularity and with simultaneous soft-story and torsional irregularities, it was concluded that the soft-story irregularity of the structure had relatively no significant effect on reaching the slight and moderate damage states. However, the extensive damage state and complete collapse of the structure were significantly affected by soft-story irregularity. Moreover, the soft-story irregularity has less effect on the 4 damage states of the buildings by increasing the number of stories. The numerical results regarding the effects of increased height on the damage extent of 3, 5 and 8-story structures are as follows:

- Damages to low-rise buildings were more affected by soft story irregularity. As the number of stories increased, the effect of soft-story irregularity on the damage state decreased. In other words, in low-rise buildings (three-story structures) the slight, moderate, extensive and complete collapse states increased to 5, 8, 9 and 4%, respectively. In mid-rise buildings (five-story structures), the slight, moderate, extensive and complete collapse states increased to 3, 4, 5 and 3%, respectively. As for the high-rise buildings (eight-story structures), the extensive and complete collapse states increased to 2 and 3%, respectively.

After examining the soft-story irregularity, the effects of torsional irregularity on the damage state of structures were examined, the results of which are summarized as follows: Torsional irregularity had no significant effect on the damage states in low-rise buildings. However, as the number of stories increased, the effect of torsional irregularity on all four damage states increased as well. Therefore, it can be said that the high-rise structures were significantly affected by torsional irregularity.

After examining the fragility curves of structures, the following numerical results were obtained:
The low-rise structures were not affected by torsional irregularity in such a way that the damage curves of the structures with torsional irregularity were completely compatible with that of the structures with regularity in plan. However, the damages to the high-rise structures were mainly attributed to the torsional irregularity. In the 8-story structure, the slight, moderate, extensive and complete collapse states increased up to 15, 12, 10 and 9%, respectively by increasing the height.

After comparing the fragility curves of 3, 5 and 8-story structures under the earthquake effects, it was concluded that the damages to the low-rise structures increased due to soft story irregularity. However, the effect of soft-story irregularity on damage states of buildings decreased by increasing the number of stories in such a way that the high-rise structures were not affected by soft-story irregularity. On the other hand, low-rise structures were not affected by torsional irregularity. But, as the number of stories increased, the damages to the structures were mostly attributed to the torsional irregularity.

The effects of soft story and torsional irregularity on the base shear-roof displacement of the structures were compared. The results indicated that in equal base shear, the extent of displacement increased 7, 9 and 11% in 3, 5 and 8 structures with torsional irregularity, respectively.

This study examined the damage states of structures with soft-story irregularity and torsional irregularity. Although some findings of previous studies especially the ones indicating that other irregularities that were mentioned in international building codes such as cutting off the lateral load system, the soft story, etc. could cause damages the buildings under earthquakes, can be considered as interesting subjects for future research, the soft-story irregularity can occur due to various reasons such as the increasing the height of the story, inappropriate usage of masonry infill walls, cutting off or removing structural elements (column or beam). In this study, the soft story irregularity was mainly attributed to the increase of height of the story. However, other factors involved in creating soft-story irregularity can be examined in future research.

15. REFERENCES

1. Pahlavan, H., Zakeri, B. and Ghodrati Amiri, G., "Probabilistic performance assessment of retrofitted horizontally curved multi-frame rc box-girder bridges", ***Journal of Earthquake and Tsunami***, Vol. 11, No. 04, (2017), 1750010, https://doi.org/10.1142/S1793431117500105
2. Kennedy, R.P., Cornell, C.A., Campbell, R., Kaplan, S. and Perla, H., "Probabilistic seismic safety study of an existing nuclear power plant", ***Nuclear Engineering and Design***, Vol. 59, No. 2, (1980), 315-338, https://doi.org/10.1016/0029-5493(80)90203-4
3. Kircher, C.A., Nassar, A.A., Kustu, O. and Holmes, W.T., "Development of building damage functions for earthquake loss estimation", ***Earthquake spectra***, Vol. 13, No. 4, (1997), 663-682, https://doi.org/10.1193/1.1585974
4. Anagnos, T., Rojahn, C. and Kiremidjian, A.S., "Nceer-atc joint study on fragility of buildings", (1995), http://hdl.handle.net/10477/700
5. Ozturk, B., Sahin, H.E. and Yildiz, C., "Seismic performance assessment of industrial structures in turkey using the fragility curves", in 15th World Conference on Earthquake Engineering, Lisbon, Portugal. (2012), 1-7.
6. Naseri, A., Pahlavan, H. and Ghodrati Amiri, G., "Probabilistic seismic assessment of rc frame structures in north of iran using fragility curves", ***Journal of Structural and Construction Engineering***, Vol. 4, (2018), 58-78, doi: 10.22065/JSCE.2017.78827.1095. .
7. Pahlavan, H., Shaianfar, M., Ghodrati Amiri, G. and Pahlavan, M., "Probabilistic seismic vulnerability assessment of the structural deficiencies in iranian in-filled rc frame structures", ***Journal of Vibroengineering***, Vol. 17, No. 5, (2015), 2444-2454, https://www.jvejournals.com/article/15794
8. Ozturk, B., "Seismic behavior of two monumental buildings in historical cappadocia region of turkey", ***Bulletin of Earthquake Engineering***, Vol. 15, No. 7, (2017), 3103-3123, https://doi.org/10.1007/s10518-016-0082-6
9. Hwang, S.-H. and Lee, K., "Probabilistic seismic demand assessment of steel moment-resisting frame buildings with ordinary and essential occupancy uses", ***International Journal of Steel Structures***, Vol. 20, (2020), 1230-1240, https://doi.org/10.1007/s13296-020-00354-0
10. Kassem, M.M., Nazri, F.M., Farsangi, E.N. and Ozturk, B., "Improved vulnerability index methodology to quantify seismic risk and loss assessment in reinforced concrete buildings", ***Journal of Earthquake Engineering***, (2021), 1-36, doi. https://doi.org/10.1080/13632469.2021.1911888
11. Fattahi, F. and Gholizadeh, S., "Seismic fragility assessment of optimally designed steel moment frames", ***Engineering Structures***, Vol. 179, (2019), 37-51, https://doi.org/10.1016/j.engstruct.2018.10.075
12. Taiyari, F., Mazzolani, F.M. and Bagheri, S., "Damage-based optimal design of friction dampers in multistory chevron braced steel frames", ***Soil Dynamics and Earthquake Engineering***, Vol. 119, (2019), 11-20, https://doi.org/10.1016/j.soildyn.2019.01.004
13. County, C., "Federal emergency management agency", ***F***EMA Community, No. 170132, (2013).
14. Abkar, G. and Lorki, A.A., "Evaluation of progressive collapse in steel structures designed based on iranian code of practice for seismic resistant design buildings (standard no. 2800), and iranian national building code'inbc', part 10", ***Journal of civil Engineering and Materials Application***, Vol. 2, No. 4, (2018), 192-200.
15. Trombly, B., "The international building code (ibc)", CMGT 564-Term Paper, (2006),.

16. ASCE, "Minimum design loads for buildings and other structures, American Society of Civil Engineers. Vol., No., (2005).
17. Malley, J.O., "The 2005 aisc seismic provisions for structural steel buildings", ***Engineering Journal-American Institute of Steel Construction***, Vol. 44, No. 1, (2007).
18. Lignos, D.G., Krawinkler, H. and Whittaker, A.S., "Prediction and validation of sidesway collapse of two scale models of a 4-story steel moment frame", ***Earthquake Engineering & Structural Dynamics***, Vol. 40, No. 7, (2011), 807-825, https://doi.org/10.1002/eqe.1061
19. Mander, J.B., Priestley, M.J. and Park, R., "Theoretical stress-strain model for confined concrete", ***Journal of Structural Engineering***, Vol. 114, No. 8, (1988), 1804-1826, doi. https://doi.org/10.1061/(ASCE)0733-9445(1988)114:8(1804)
20. Li, Y., Song, R. and Van De Lindt, J.W., "Collapse fragility of steel structures subjected to earthquake mainshock-aftershock sequences", ***Journal of Structural Engineering***, Vol. 140, No. 12, (2014), 04014095, https://doi.org/10.1061/(ASCE)ST.1943-541X.0001019
21. Banazadeh, M. and Jalali, S.A., "Probabilistic seismic demand assessment of steel moment frames with sideplate connections", ***Amirkabir Journal of Civil Engineering***, Vol. 44, No. 2, (2013), 47-64, https://doi.org/10.1016/j.scient.2011.11.036

16. APPENDIX

The specifications of the sections used in this research for three-, five-, and eight-story structures are specified in Tables 3 to 11(The beam sections are I-shaped and the column sections are box-shaped). For example, a beam with dimensions of 20 * 18 * 1 means a beam with a height of 20 and a width of 18 and a thickness of 1 cm, and a column with dimensions of 20 * 20 * 1 means a column with dimensions of 20 by 20 and a thickness It is 1 cm. Figure 26 shows the plan of the structures, that the type of beams is specified by color.

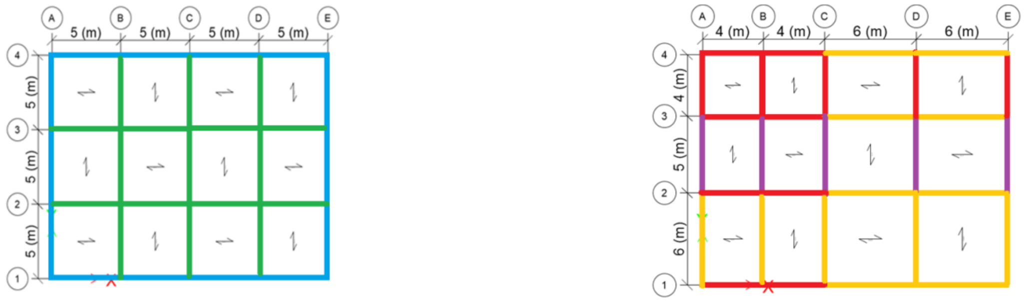

(a) (b)

Figure 26. The plan of different types of modeled structures: (a) Structure with regular plan; (b) Structure with an Irregular plan

TABLE 3. The specifications of the sections for three-story with soft story

Number of story	Beam selected by green color	Beam selected by blue color	column 1-A, 1-B, 1-C, 1-D, 1-E 2-A, 2-D 3-A, 3-D 4-A, 4-B, 4-C, 4-D, 4-E	column 2-B, 2-C, 2-D 3-B, 3-C, 3-D
1	20*18*1	20*16*0.8	27*27*1	22*22*1
2	20*18*1	20*16*0.8	25*25*0.8	20*20*0.8
3	20*18*1	20*16*0.8	25*25*0.8	20*20*0.8

TABLE 4. The specifications of the sections for three-story with torsional irregularity in plane

Number of story	Beam selected by red color	Beam selected by yellow color	Beam selected by purple color	Column 1-A, 1-B, 1-C, 1-D, 1-E	Column 2-A, 2-B, 2-C, 2-D, 2-E 3-A, 3-B, 3-C, 3-D, 3-E	Column 4-A, 4-B, 4-C, 4-D, 4-E
1	15*15*0.5	20*15*0.8	15*15*0.8	30*30*0.8	25*25*0.8	25*25*0.5
2	15*15*0.5	20*15*0.8	15*15*0.8	30*30*0.8	25*25*0.8	25*25*0.5
3	15*15*0.5	20*15*0.8	15*15*0.8	25*25*0.8	20*20*0.8	15*15*0.5

TABLE 5. The specifications of the sections for three-story with simultaneous soft story and torsional irregularity

Number of story	Beam selected by red color	Beam selected by yellow color	Beam selected by purple color	Column 1-A, 1-B, 1-C, 1-D, 1-E	Column 2-A, 2-B, 2-C, 2-D, 2-E 3-A, 3-B, 3-C, 3-D, 3-E	Column 4-A, 4-B, 4-C, 4-D, 4-E
1	15*15*0.5	20*15*0.8	15*15*0.8	32*32*1	30*30*1	28*28*0.8
2	15*15*0.5	20*15*0.8	15*15*0.8	30*30*0.8	25*25*0.8	25*25*0.5
3	15*15*0.5	20*15*0.8	15*15*0.8	25*25*0.8	20*20*0.8	15*15*0.5

TABLE 6. The specifications of the sections for five-story with soft story

Number of story	Beam selected by green color	Beam selected by blue color	column 1-A, 1-B, 1-C, 1-D, 1-E 2-A, 2-D 3-A, 3-D 4-A, 4-B, 4-C, 4-D, 4-E	column 2-B, 2-C, 2-D 3-B, 3-C, 3-D
1	22*20*1	20*16*1	30*30*1.2	32*32*1.2
2	22*20*1	20*16*1	28*28*1	30*30*1
3	20*16*0.8	18*16*0.8	22*22*1	26*26*1
4	20*16*0.8	18*16*0.8	22*22*1	26*26*1
5	18*16*0.8	16*16*0.8	18*18*0.8	20*20*0.8

TABLE 7. The specifications of the sections for five-story with torsional irregularity in plane

Number of story	Beam selected by red color	Beam selected by yellow color	Beam selected by purple color	Column 1-A, 1-B, 1-C, 1-D, 1-E	Column 2-A, 2-B, 2-C, 2-D, 2-E 3-A, 3-B, 3-C, 3-D, 3-E	Column 4-A, 4-B, 4-C, 4-D, 4-E
1	20*15*0.8	25*20*1	20*15*0.8	40*40*1.4	36*36*1.2	30*30*1
2	20*15*0.8	25*20*1	20*15*0.8	40*40*1.4	36*36*1.2	30*30*1
3	18*15*0.8	22*18*0.8	18*15*0.8	32*32*1.4	30*30*1.2	25*25*1
4	18*15*0.8	22*18*0.8	18*15*0.8	32*32*1.4	30*30*1.2	25*25*1
5	16*15*0.8	20*16*0.8	16*15*0.8	20*20*0.8	20*20*0.8	20*20*0.8

TABLE 8. The specifications of the sections for five-story with simultaneous soft story and torsional irregularity

Number of story	Beam selected by red color	Beam selected by yellow color	Beam selected by purple color	Column 1-A, 1-B, 1-C, 1-D, 1-E	Column 2-A, 2-B, 2-C, 2-D, 2-E 3-A, 3-B, 3-C, 3-D, 3-E	Column 4-A, 4-B, 4-C, 4-D, 4-E
1	20*15*0.8	25*20*1	20*15*0.8	44*44*1.6	40*40*1.4	32*32*1.2
2	20*15*0.8	25*20*1	20*15*0.8	40*40*1.4	36*36*1.2	30*30*1
3	18*15*0.8	22*18*0.8	18*15*0.8	32*32*1.4	30*30*1.2	25*25*1
4	18*15*0.8	22*18*0.8	18*15*0.8	32*32*1.4	30*30*1.2	25*25*1
5	16*15*0.8	20*16*0.8	16*15*0.8	20*20*0.8	20*20*0.8	20*20*0.8

TABLE 9. The specifications of the sections for eight-story with soft story

Number of story	Beam selected by green color	Beam selected by blue color	column 1-A, 1-B, 1-C, 1-D, 1-E 2-A, 2-D 3-A, 3-D 4-A, 4-B, 4-C, 4-D, 4-E	column 2-B, 2-C, 2-D 3-B, 3-C, 3-D
1	40*20*1	40*20*0.8	44*44*1.2	44*44*1.4
2	40*20*1	40*20*0.8	40*40*1.2	40*40*1.4
3	32*18*1	32*16*0.8	40*40*1.2	40*40*1.4
4	32*18*1	32*16*0.8	35*35*0.8	35*35*1
5	32*18*1	32*16*0.8	35*35*0.8	35*35*1
6	20*15*0.8	20*15*0.6	35*35*0.8	35*35*1
8	20*15*0.8	20*15*0.6	16*16*0.8	16*16*1
9	20*15*0.8	20*15*0.6	16*16*0.8	16*16*1

TABLE 10. The specifications of the sections for eight-story with torsional irregularity in plane

Number of story	Beam selected by red color	Beam selected by yellow color	Beam selected by purple color	Column 1-A, 1-B, 1-C, 1-D, 1-E	Column 2-A, 2-B, 2-C, 2-D, 2-E 3-A, 3-B, 3-C, 3-D, 3-E	Column 4-A, 4-B, 4-C, 4-D, 4-E
1	40*20*0.8	40*20*1	40*20*0.8	44*44*1.4	40*40*1.4	40*40*1
2	40*20*0.8	40*20*1	40*20*0.8	44*44*1.4	40*40*1.4	40*40*1
3	40*20*0.8	40*20*1	40*20*0.8	44*44*1.4	40*40*1.4	40*40*1
4	32*18*0.8	36*18*0.8	32*18*0.8	36*36*1	35*35*1	32*32*1
5	32*18*0.8	36*18*0.8	32*18*0.8	36*36*1	35*35*1	32*32*1
6	32*18*0.8	36*18*0.8	32*18*0.8	36*36*1	35*35*1	32*32*1
7	20*0.6*15*0.6	20*15*0.8	20*0.6*15*0.6	20*20*1	18*18*1	16*16*1
8	20*0.6*15*0.6	20*15*0.8	20*0.6*15*0.6	20*20*1	18*18*1	16*16*1

TABLE 11. The specifications of the sections for eight-story with simultaneous soft story and torsional irregularity

Number of story	Beam selected by red color	Beam selected by yellow color	Beam selected by purple color	Column 1-A, 1-B, 1-C, 1-D, 1-E	Column 2-A, 2-B, 2-C, 2-D, 2-E 3-A, 3-B, 3-C, 3-D, 3-E	Column 4-A, 4-B, 4-C, 4-D, 4-E
1	40*20*0.8	40*20*1	40*20*0.8	44*44*1.6	44*44*1.4	44*44*1
2	40*20*0.8	40*20*1	40*20*0.8	44*44*1.4	40*40*1.4	40*40*1
3	40*20*0.8	40*20*1	40*20*0.8	44*44*1.4	40*40*1.4	40*40*1
4	32*18*0.8	36*18*0.8	32*18*0.8	36*36*1	35*35*1	32*32*1
5	32*18*0.8	36*18*0.8	32*18*0.8	36*36*1	35*35*1	32*32*1
6	32*18*0.8	36*18*0.8	32*18*0.8	36*36*1	35*35*1	32*32*1
7	20*0.6*15*0.6	20*15*0.8	20*0.6*15*0.6	20*20*1	18*18*1	16*16*1
8	20*0.6*15*0.6	20*15*0.8	20*0.6*15*0.6	20*20*1	18*18*1	16*16*1

Persian Abstract

چکیده

در این پژوهش، منحنی‌های شکنندگی برای سازه‌های فولادی قاب خمشی با تعداد طبقات سه، پنج و هشت که نماینده سازه کوتاه، متوسط و بلندمرتبه است و همچنین دارای نامنظمی طبقه نرم و نامنظمی پیچشی در پلان می‌باشد، توسعه داده‌شده است. این مدل‌ها بر اساس آیین‌نامه ایران طراحی‌شده‌اند و به‌صورت سه‌بعدی در نرم‌افزار OpenSees تحت تحلیل دینامیکی افزایشی (IDA) گرفته و منحنی‌های IDA برای آن‌ها محاسبه‌شده است. مقدار حداکثر نسبت دیریفت به‌عنوان پارامتر تقاضا بر اساس آیین‌نامه HAZUS-MH انتخاب شد و درنهایت، منحنی‌های شکنندگی مربوطه توسعه داده شد. نتایج تجزیه و تحلیل دینامیکی غیرخطی نشان داد که با افزایش تعداد طبقات، آسیب ناشی از نامنظمی طبقه نرم کاهش می‌یابد. از طرف دیگر، آسیب ناشی از نامنظمی پیچشی در پلان با افزایش تعداد طبقات افزایش می‌یابد.